CONFIDENTIAL

Internship report

Preforming process simulation

Dennis Brands

s1087630

22nd September 2014

–

20th May 2015

University of Twente

CTW, OPM-PT

Prof. Dr. Ir. Remko Akkerman

Audi AG

N/PG-A33

Wojciech Brymerski

Neckarsulm, Germany

UNIVERSITY OF TWENTE.

Confidentiality Note

Publications about the content of this document require the written consent of the AUDI AG in advance.

The results, opinions and conclusions expressed in this document are not necessarily those of the AUDI AG.

This document is classified "internal". It is to be made accessible only

- inside the Volkswagen Group,
- the responsible person at the university/college and
- to the correctors as well as
- to the members of the examining board.

The responsible person at the university/college, correctors and members of the examining board are to be obliged to secrecy in advance.

The report is strictly confidential and will remain inaccessible to any other parties outside the agreed confidentiality loop for a period of five years.

Table of Content

1. Introduction

Composite materials and in particular fibre reinforced plastics have gained popularity in engineering over the last few decades. The high specific modulus achievable with glass or carbon fibres in a thermoplastic or thermosetting matrix provides a potential weight saving when compared to lightweight metals. In the aviation industry composite material have already gained acceptance and is currently applied at an industrial scale. The automotive industry however is still struggling to apply these materials due to added cost and long cycle times. Material suppliers are therefore developing new materials that enable possibilities in part production with lower cycle times and reduced cost, in return the performance is often less than that of aviation grade material. Mitsubishi Pyrofil developed by Mitsubishi Rayon is a uni-directional (UD) carbon fibre prepreg with an epoxy matrix. The blend of epoxy has been developed for fast out of autoclave curing in a heated press. The material also has a long shelf life in storage, can be kept at room temperature for a relatively long time, has good properties for handling at room temperature, improved formability at an elevated temperature without curing and will cure in a few minutes at the curing temperature. All properties which contribute to low cycle times and the ability for automated processing.

This chapter describes a new preforming process developed at Audi and the process simulation thereof in Pam-Form. The layers of material are cut, stacked, the large deformations are realized using preforming and the preform is than consolidated and cured at elevated temperature and pressure in an industrial press to obtain the ready part. This process should not take more than several minutes for it to be economically viable for Audi. The preforming stage is important since defects like wrinkles often arise during this stage.

Process simulation is applied to enable the prediction of defects and study the behaviour of the process. The knowledge gained can be used to improve the principle of the process or improve tooling geometry for new parts. The geometry used is a part specifically for testing the new process and the simulation will be compared and calibrated to the real forming attempts on this part.

First a description of the process is given, thereafter the input for the simulation in Pam-Form is described before the simulation results are presented. Thereafter an analogue simulation is described and performed in AniForm. Conclusions for both simulation attempts are given. Lastly a pressing process with rigid tooling is studied as a comparison to the preforming process presented in the beginning of the report.

2. Process description

Before the process steps can be presented a brief introduction into the preforming equipment is given. In Figure 1 the equipment is show with numbering that corresponds to the list with a description for each part:

(1) Tool that provides the shape of the part made of steel. Vacuum is applied to the tooling and the table.
(2) Rubber membrane spanned in a frame. The rubber was specially designed for vacuum forming processes in production of composite parts. The frame is hinged on the bottom side and is able to turn 180° around that axis.
(3) Prepreg stack which sticks to the membrane. It is heated using a contact heating element on one side before being formed.

Additional tooling around the steel mould can be present. This tooling will not be in contact with any prepreg and is only there to influence the movement of the membrane.

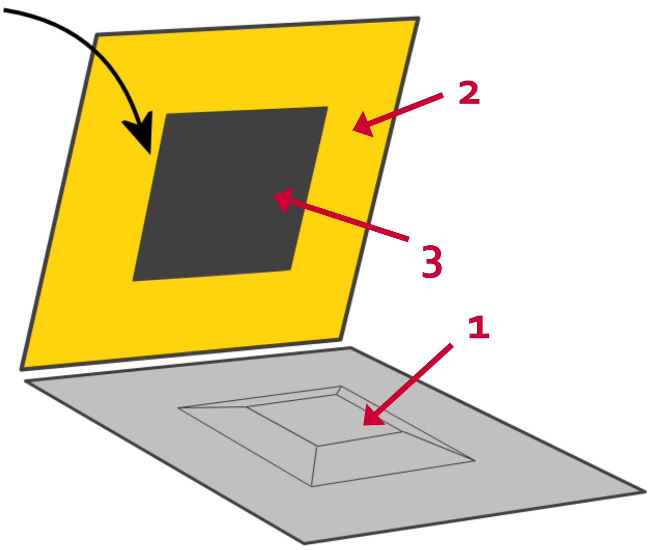

Figure 1: Schematic representation of the preforming equipment

The preforming process is comprised of different steps as described below. The layup of the part will be formed in three separate steps. First the stack (0°/90°) is preformed, then on top of that the stack $(+45°/-45°)_s$ is formed and finally a stack of (90/0) is formed to make the quasi-isotropic layup of $(0°/90°/+45°/-45)_s$. The stacks are so called sequentially shaped for better formability.

1. The material is cut to size and from the larger role of material.
2. Foil and backing paper are removed and the layers are stacked as desired. Most air is removed by smoothing and pressing the layers together.
3. The stack is placed on the predetermined spot on the membrane. The heating element is directly below the part of the membrane where the stack is placed.
4. When the stacked is heated the frame is turned over to the other side. The stack will stick to the membrane due to tackiness.

5. When the frame with the membrane reaches the table surface the vacuum will shape the membrane, along with the stack, over the tooling, thereby preforming the stack to the desired shape.
6. Steps III-V can be repeated with different stacks to build up the preform.
7. Vacuum is removed and membrane can be pulled from the tooling whilst rotating the frame back to its original position.
8. Preformed stack is removed from the tooling by applying pressured air to the vacuum channels in the steel tooling.

3. Preforming of C/Epoxy UD prepreg using a flexible membrane – simulations in Pam-Form

In this chapter the process simulation in Pam-Form is described. It starts with the pre-processing for the membrane material and related settings. Thereafter the characterization of some material values for the C/Epoxy UD is explained. The results obtained using the Pam-Form program are presented last.

3.1. CAD geometry and meshing

Since the actual deformation of the composite material is of interest only the last stage of the preforming process is modelled in which the composite deforms. The frame with the membrane in the beginning of the simulation is in the position just before it touches the tooling.
Two situations are simulated. One without the foam model in which the real process gives many wrinkles and another with the foam tooling by which the wrinkles were minimized. Meshed geometries are shown in Figure 2. The frames have to be rotated another 11° and 18° respectively in the simulation. The tooling surface mesh was adopted from the CAD geometry of the toolmaker. The foam tooling was modelled by eye from images of the process and also meshed as a surface. The blanks were meshed with 4422 rectangular elements of length 5. The membrane was meshed with 17956 rectangular elements also with length 5. The frame is modelled by making the outer nodes of the membrane a rigid body and rotating them around one edge.

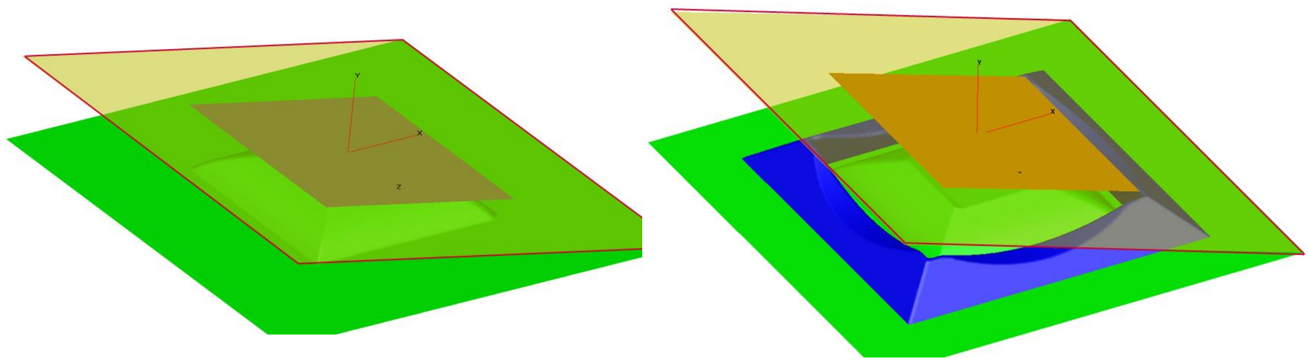

Figure 2: Two meshed geometries that show the beginning of the simulation. Membrane is made transparent. Frame is the edge nodes from the membrane and are made red in the image for clarity.

3.2. Modelling of the flexible membrane

3.2.1. Material model by Ogden

Material parameters for the membrane are not supplied by the manufacturer at this time. Only the strain at fracture of 800% is a given, therefore a material model for large strains is needed. Pam-Form will be used for the simulation and therefore it can only be modelled using an Ogden model or a G'Sell-Jonas model. In order to avoid having to do a lot of experiments the alternative of finding a model in literature is considered. A ready fitted Ogden model for unfilled silicone rubber was found in work of Meunier (1). It is estimated that this is similar to the material at hand.

The Ogden model like many hyperelastic material models is expressed as a strain energy density function. It is described in terms of the principle stretches using the N μ_p α_p as material constants in:

$$W(\lambda_1, \lambda_2, \lambda_3) = \sum_{p=1}^{3} \frac{\mu_p}{\alpha_p} (\lambda_1^{\alpha_p} + \lambda_2^{\alpha_p} + \lambda_3^{\alpha_p} - 3)$$

This model can describe stress-strain behaviour of complex materials like rubbers and polymers that show no strain-rate dependence. For certain choices of N and alpha's the model reduces to the neo-Hookean model or the Mooney Rivlin model. A choice of N=3 can capture the non-linear behaviour of rubbers very well. The values found by Meunier et al. (1) are found in Table 1.

α_1	1.4	μ_1	0.46 MPa
α_2	10	μ_2	0.00027 MPa
α_3	-3.3	μ_3	-0.0074 MPa

Table 1: Ogden model coefficients for silicone rubber found by Meunier et al. (1)

The model will be visualized using a 1D approach with use of the uni-axial stress related to the stretch ratio defined as l/l_0. Assumptions made are $\sigma_2 = \sigma_3 = 0$ and incompressibility.

$$\sigma_j = \sum_{p=1}^{N} \left(\mu_p {\lambda_j}^{\alpha_p} - \mu_p {\lambda_j}^{-0.5\alpha_p}\right)$$

Using this relation and relation for engineering strain $\varepsilon = \lambda - 1$ the traditional engineering stress-strain is plotted in Figure 3. This figure is readily comparable to figure 10a from the original paper and is in good agreement. It can be seen that the material has an initial stiffness of 0.5 MPa and stiffness increases rapidly after 100% strain.

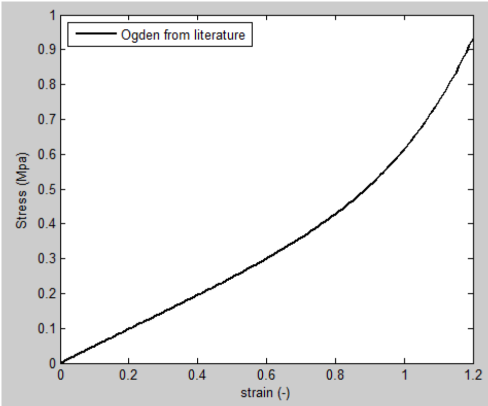

Figure 3: Engineering stress-strain plot for silicon rubber with values by Meunier et al. (1)

Using this material model in combination with simulation was however unsuccessful due to stability issues in Pam-Form. An increased stiffness as will be described later also was no solution to this problem. Next a different model based on the same values will be used which will not show stability issues.

3.2.2. Material model by G'sell–Jonas

A second possibility to model the rubber would be using the G'sell-Jonas model originally developed for the elastic-viscoplastic behaviour of semi-crystalline polymers. This phenomenological model uses multiplicative terms to describe the true stress-strain behaviour including strain rate dependency at small and large strains. The stress is expressed as:

$$\sigma(\epsilon,\dot{\epsilon}) = k \cdot (1 - e^{-w\epsilon}) \cdot e^{h\epsilon^2} \cdot \left(\frac{\dot{\epsilon}}{\dot{\epsilon}_0}\right)^m$$

In this relation k is a scaling factor. The term $(1 - e^{-w\epsilon})$ describes the visco-elastic behaviour for small strains. (Since the term $e^{h\epsilon^2} \sim 1, \epsilon \ll 1$). The $e^{h\epsilon^2}$ term describes the strain hardening effect. The last term $\left(\frac{\dot{\epsilon}}{\dot{\epsilon}_0}\right)^m$ captures the strain-rate sensitivity. The term $\dot{\epsilon}_0$ is there for homogeneity and is 1 s^{-1}.

Since silicone rubber shows little to no strain rate dependence for the speeds considered in this forming process the value of parameter **m** is set to 0. The stiffness for small strains, or initial stiffness, is then the product of **k** and **w**.

It was found that the stability of the simulation is better when an initial stiffness of 10 MPa is used, therefore the values of μ in the Ogden model are multiplied by 20. With a higher value for the stiffness of the membrane the stability of the calculation is improved. The author believes that this value is still low enough compared to the stiffness of the composite to model the process properly.

Now the values of **k**, **w** and **h** in the G'sell model are adapted to approximate the Ogden model in the uni-axial tensile test over a certain range. The result is shown in Figure 4.

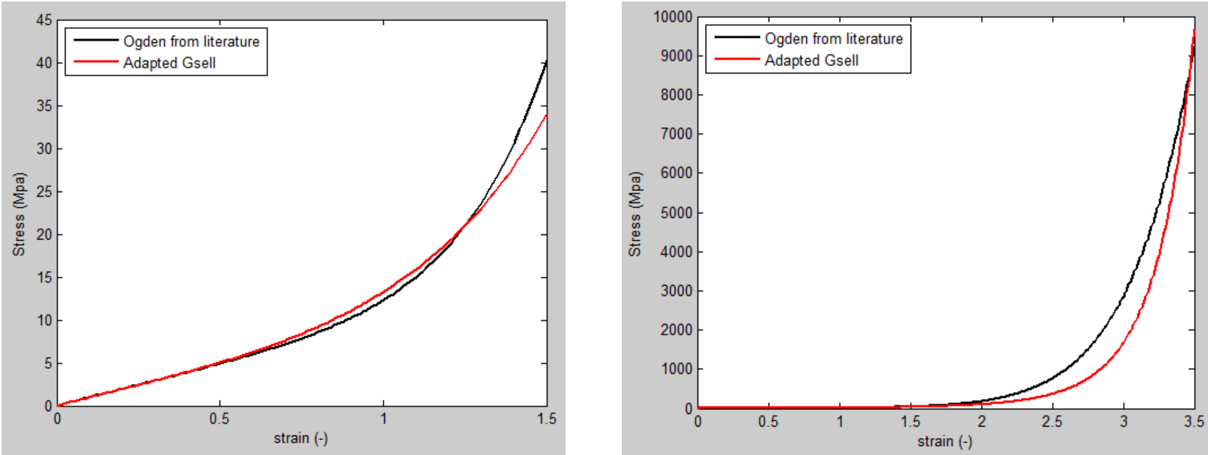

Figure 4: Comparison of adapted Ogden and G'Sell model.

It is observed that the initial stiffness in the uni-axial tensile test is indeed 10 MPa, the model are in good agreement up to 150% strain and the G'sell could be used up to about 350% strain. After 350% strain the stresses become too large due to the higher stiffness in the G'sell model.

It was found that with these values for the G'sell model a simulation without significant stability issues can be performed. Why an Ogden model with theoretically the same initial stiffness does show these problems is not fully understood by the author.

3.2.3. Simulation time and inertia

From initial test simulations it was found that the membrane can show problems with inertia. The frame is favourably moved at a high speed to keep simulation times low. However due to the low stiffness of the membrane this will give unreal results. Figure 5 shows a simulation with the membrane only. The size, elements and rotation is the same as in the process simulation. The left picture shows problems using the real density of the material. On the right the density is several orders lower and the inertia problem is not observed anymore. The speed used in the simulation was aimed at providing a simulation that solves in a matter of hours, instead of days.

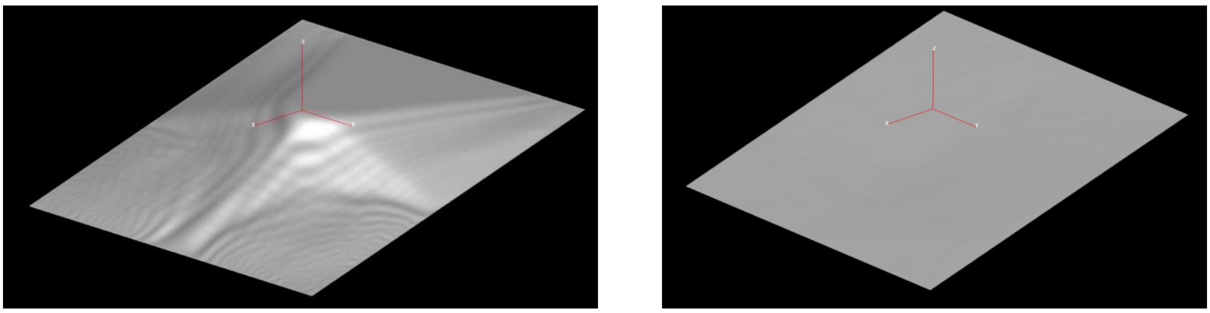

Figure 5: Simulation of the membrane only, where the edge is rotated. Left shows problems using normal density, right with lowered density does not have this problem.

In the previous section the density of the membrane was lowered to overcome inertia problems, however the same has to be done for the composite material since it will be attached to the membrane during the simulation. Lowering the density on the composite however provides longer simulation times due to conditional stability in explicit finite element method (FEM) (2). The critical time step is expressed as:

$$\tau = \frac{l \cdot \rho}{E}, l = typical\ element\ edge\ length, \rho = density,\ E = stiffness$$

The formula above shows that that lowering the density lowers the critical time step. This can be overcome by equally lowering the stiffness of these elements. Therefore, by lowering both the density of composite and membrane and also lowering the highest stiffness in the composite, we are able to have simulations without inertia problems in decent times. The highest stiffness in the composite was originally modelled as 100 GPa and could therefore be lowered. Care has to be taken that this value remains large when compared to the other stiffness's in the composite material.

Using the material model above and having paid attention to the densities and stiffness's it was possible to model the first part of the process, which is the turning of the frame onto the mould with membrane and composite. An image of the result is shown in Figure 6.

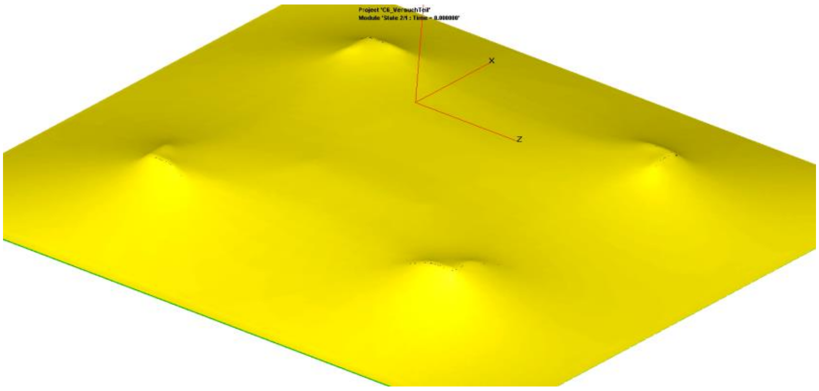

Figure 6: Result after moving the membrane with composite over the mould.

In the next section the application of a vacuum on the membrane in simulation is presented.

3.3. Modelling of vacuum

3.3.1. Pressure curve

During preforming the air is taken out from underneath the membrane, thereby creating a pressure difference over the membrane. The pressure difference will form the membrane and composite over the mould. In the simulation the pressure difference is modelled as a pressure force on the outside of the membrane. No data is available on the application of the vacuum, therefore it is estimated that it is applied uniformly over the membrane. When a full vacuum is applied a pressure difference of 1 bar or 0.1 MPa is achieved. This is a theoretical maximum for the loading.

In initial test simulations it was found that an instant application of 0.1 MPa of pressure is not possible due to stability issues. Therefore a parallel adjustment of the pressure application curve and the damping parameters (see section Damping 3.3.2) was made. It was found that a slow and linear application of the pressure can lead to stable simulation, however to observe the closing of the membrane best in the results and to have short simulation times a ramp curve works best. An example of a pressure curve used can be found in
Figure 7.

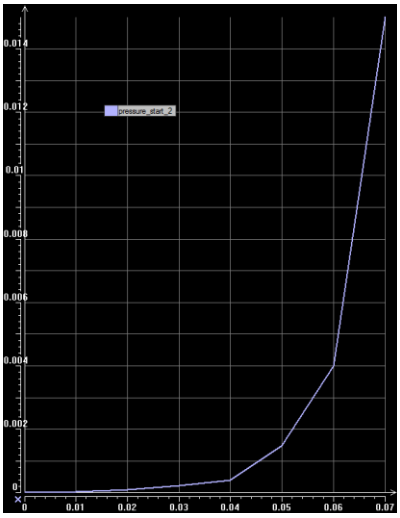

Time (s)	Pressure (MPa)
0	0
0.01	0.000025
0.02	0.000099
0.03	0.000222
0.04	0.000394
0.05	0.0015
0.06	0.004
0.07	0.009
0.08	0.018
0.09	0.03
0.1	0.048

Figure 7: Pressure curve for time in seconds and pressure in MPa.

In the simulation it is often sufficient to not simulate full vacuum but to stop at the moment the membrane has closed the entire mould. This value for the pressure has to be determined by experience or an initial simulation. By not applying the full vacuum the contact stiffness's also needn't be as high, this is beneficial for simulation time.

3.3.2. Damping

Whilst initial simulations were performed it was found that applying a pressure on a very compliant substrate gives very fast dynamic behaviour in the material, leading to very high speeds. These speeds are a source of instability and provide difficulty in contact. This dynamic behaviour also does not describe the bulk of the behaviour and is therefore unnecessary in the model. Damping was added to the simulation in order to stabilize and speed up calculation. Three sources of damping were added: Nodal damping, contact damping and strain-rate filtering.

Nodal damping is added according to $f = m \cdot q \cdot v$ in which a force is added proportional to mass, velocity and q with the dimension of time^{-1}. A single frequency of $q = 2\omega$ is critically damped while other frequencies are partially damped. Contact damping is added as Rayleigh damping proportional to stiffness. The material cards for the membrane and the composite also provide a possibility for strain-rate filtering over a certain amount of time steps, this will eliminate extremities in terms of strain rate and will therefore prevent very stiff and very compliant elements next to each other, again stabilizing the simulation.

Values for damping should be chosen carefully to avoid influencing the large deformations. The result of the latter is depicted in Figure 8.

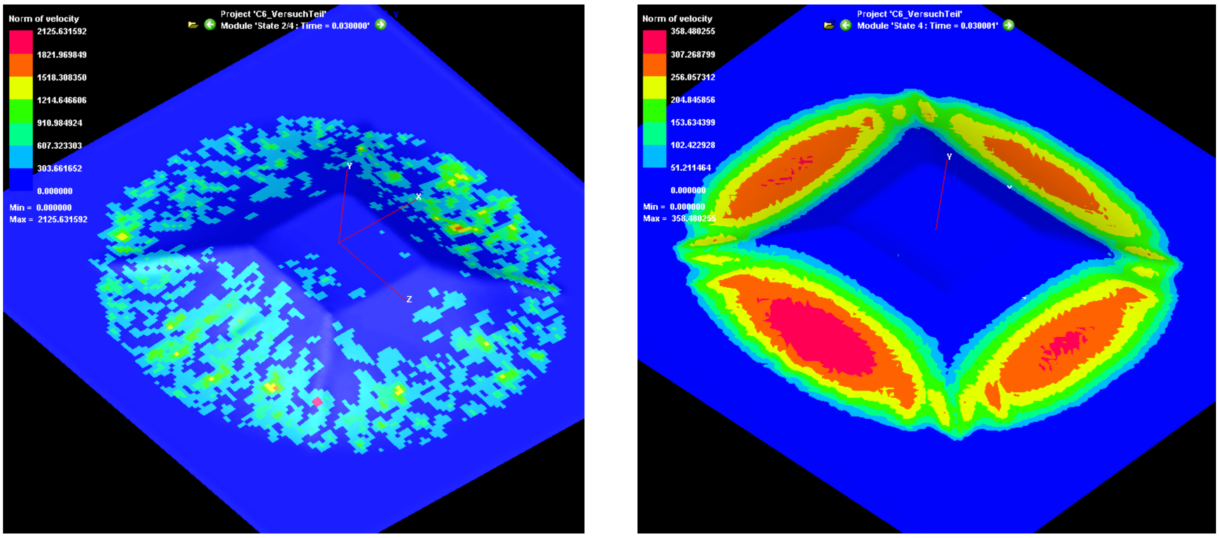

Figure 8: The velocity result of adding damping to the simulation. Maximum velocities are 2125 and 358 mm/s respectively for the left without damping and the right with damping.

Using the material model for the membrane, reduced densities and stiffness's, a ramped pressure curve and after added damping the full process can be simulated in Pam-Form. The result of a fully closed membrane is shown in Figure 9. In the next section a material model for the composite will be researched that provides flaws similar to reality.

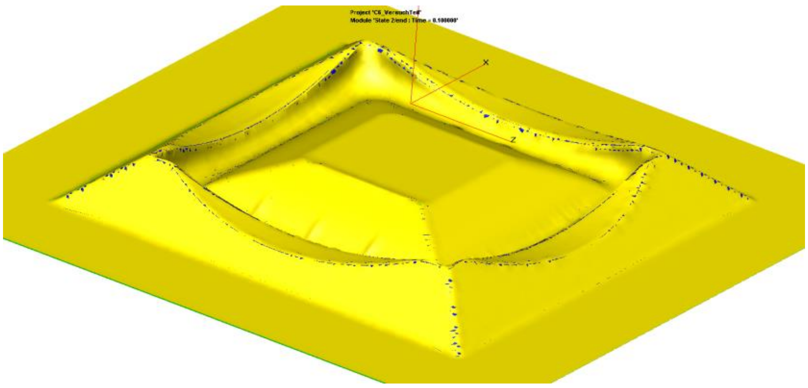

Figure 9: Resulting closed membrane after applying the pressure in the simulation.

3.4. Material characterisation of C/Epoxy UD prepreg

For a process simulation to be used as a predictive tool the results should show similarity to the real process. A good material model for the composite is important when trying to predict a preforming process. In simulating the draping of a composite a few characteristic deformation mechanisms have been recognized in previous research. The most dominant being (longitudinal) intra-ply shear, out of plane bending and inter ply slip. The three mechanisms are depicted in Figure 10.

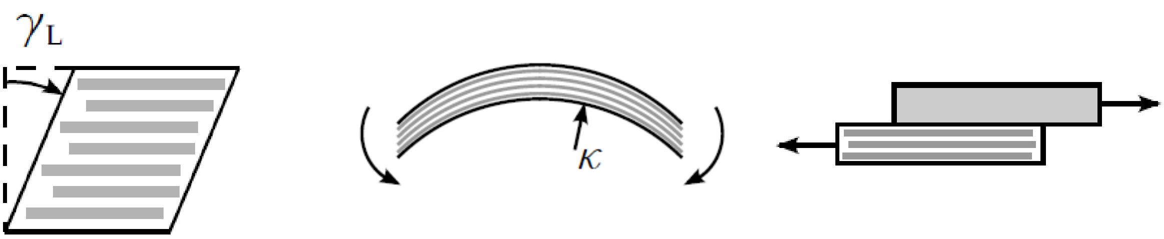

CONFIDENTIAL

Figure 10: From left to right the three most important mechanisms in composite draping: longitudinal intra-ply shear, out of plane bending and inter-ply slip.

Furthermore the material model also needs values for Young's Moduli in fibre direction and the direction perpendicular to that. And besides the inter-ply properties also properties between composite and tooling is needed.

A summary of values needed and how they were acquired is given below:

- Young's moduli E_1 (fibre direction) and E_2 (perpendicular) are estimated by experience. E_1 will be very stiff compared to E_2 and the other mechanisms. E_2 should be estimated based on the other mechanisms.
- Intra-ply shear was characterized using a torsion bar test adapted from similar test on thermoplastic matrix materials by Haanappel et al. (3)
- Bending characterization was done using the method developed by Sachs et al. (4) for thermoplastic composites.
- Both ply-ply and tool-ply friction properties have been estimated from simulation experience.

In the next sections only the method of characterization for intra-ply shear and out of plane bending will be illustrated.

3.4.1. Intra-ply shear characterization

The shear characterization on UD materials is difficult or hard to perform using conventional methods developed for fabric materials. For the characterization of intra-ply shear a test developed for thermoplastic composites in melt as developed by Haanappel et al. (3) will be used. This test is normally performed at temperatures near the melt temperature of the thermoplastic, however it will now be used at the preforming temperature of the C/Epoxy prepreg at hand. Previous experience and DSC measurements have shown that the material shows little to no crosslinking at the temperatures and for the duration of the test. Some images of what the test looks like are given in Figure 11.

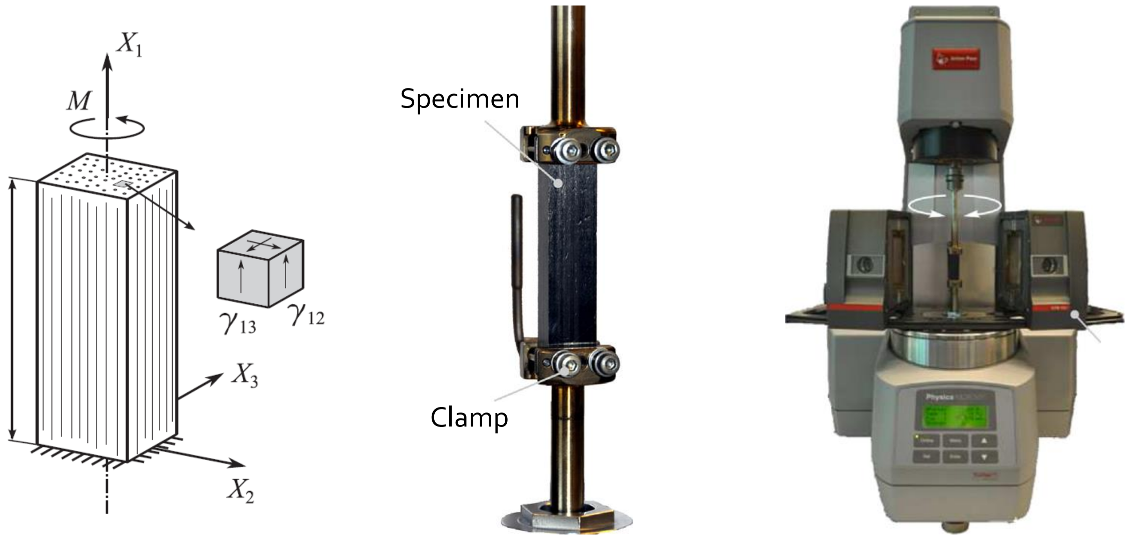

Figure 11: Images of the torsion bar shear characterization test. From left to right: schematic, torsion bar and fixture, Anton Paar MCR501 rheometer.

The torsion bar with dimensions 60x13x11mm was fabricated in house at Audi. First 72 layers of material were cut from the bulk role using an industrial cutter. These layers were then stacked by hand to form the bar shape. Each layer was pressed, whilst trying to have the least amount of air entrapments in between the layers. In total 3 specimens were fabricated each with a tolerance of ±0,1mm. The height the specimen was consistent with 72 layers of consolidated material, which indicates a small amount of air entrapments.

The specimen is clamped in the rheometer as seen in the middle image of Figure 11. This fixture is enclosed in an oven with inert gas as seen in the rightmost image of Figure 11.

A transient torsion test into the large strain regime was conducted, which is different from the original dynamic small strain shear test. On all three specimens, tests were conducted at three different speeds. Also test were repeated on each specimen, since it is known that the first test on each specimen is different from the tests thereafter. Two specimens gave similar results, whilst one specimen gave consistently higher torque values. Although the reason is unknown to the author, two possibilities come to mind: first the layup was done by two different people, second being that the clamping of the specimen was also done by two different people. Air entrapments were also not ruled out and could therefore still have influence.

From these two specimens the last three measurements were used, so for each speed two measured curves were available. These curves were interpolated on a certain time interval and then averaged to give a single curve for each measured speed. The curves are depicted on the left of Figure 12.

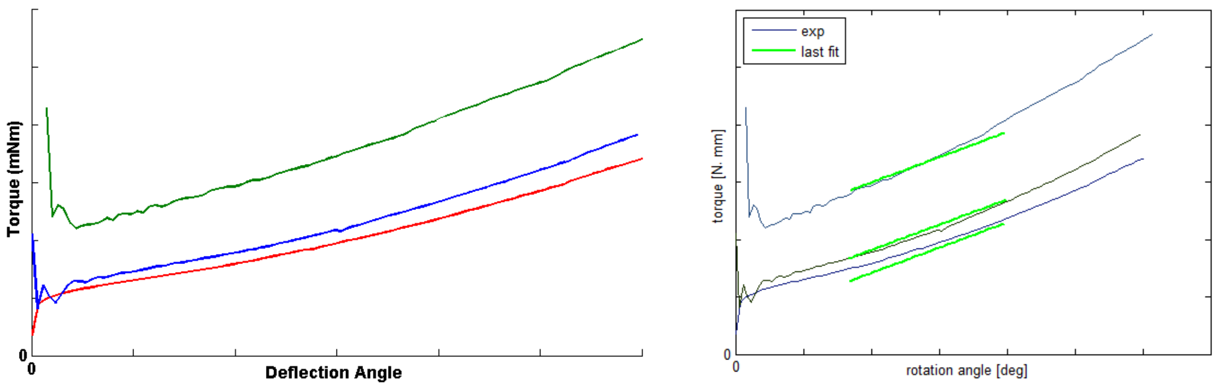

Figure 12: Measured curves for three speeds on the left, the material model fitted to this data is plotted in green in the right figure.

The curves were used inside a fitting script which could be used for this purpose very kindly supplied by the thermoplastic composite research center. This script uses the free torsion (warping included) assumption for kinematics and a Gaussian integration scheme to mathematically perform the torsion test. A material model or combination of models is chosen and a fitting procedure is used to find the optimal values so that the resulting curves match the measurements. The final iteration using an elastic model in combination with a cross-Carreau viscous model is shown on the right of Figure 12. The values found using this fitting procedure can then be used in simulation software.

Later it will be found that the measured values do not give satisfying results in the Pam-Form simulation and by trial and error it is found that a much higher stiffness, without the viscous effects does give simulation results that look more like the real tests. So unless stated otherwise the measured values are not used for the Pam-Form calculation but still used for the AniForm calculation.

3.4.2. Bending characterization

Bending characterization was done at the University of Twente using a custom build fixture for the Anton Paar MCR501 rheometer. An image showing the specimen and fixture in the rheometer is given in Figure 13. The test method was adopted from the work of Sachs et al. (4). In total 3 specimens were tested at a single speed at forming temperature. Specimen dimensions were 35x25mm and 8 plies in thickness. To manufacture the specimens 8 layers of 200x200mm were stacked by hand whilst trying to prevent air inclusions. Both surfaces were laid on glass plates and a weight of 20kg was placed on there for 30 minutes. Thereafter the specimens were cut from the plate using a carpet knife with the fibre direction along the long edge of the specimen.

Figure 13: Bending test set-up at the University of Twente as developed by Sachs et al. (4)

Again 2 specimens showed similar results, however the one specimen gave consistent lower values for torque. No explanation is given in this report for this finding. The result are again similar to curves found for thermoplastic composites in melt, for which the test was developed.

From previous measurements on thermoplastic composite it is know that the response is near linear for changing thickness, hence no classic pure bending is observed. This assumption is also taken on here, the torque is divided by 8 to obtain the approximate response for a single layer. This is then plotted for the apparent curvature if the specimen had pure bending kinematics. The curves obtained are shown in Figure 14.

From these curves a stiffness on the large strain spectrum of the measurement was determined. This could be done using a similar fitting procedure as described for the shear tests, however here it was compared to previously measured and fitted data to obtain the stiffness value. Because only a single speed was considered no good fit for a viscous model could be performed. However a constant value for viscosity could be found by comparison to previous measurements on other materials.

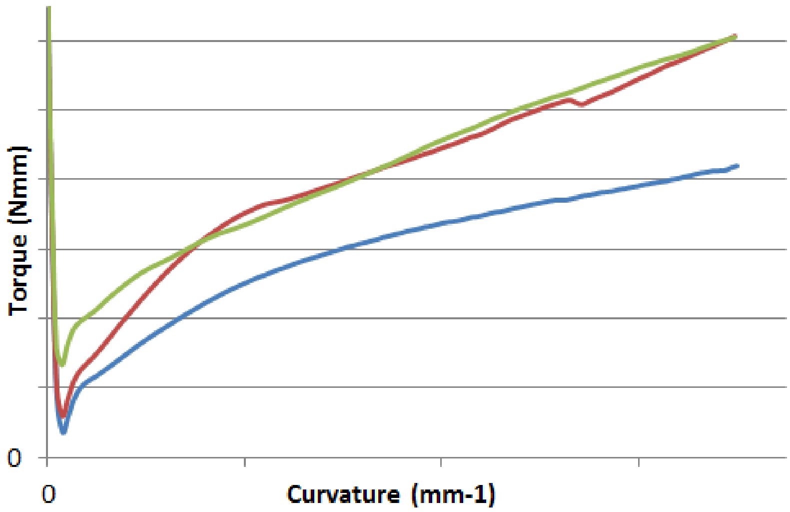

Figure 14: Curves measured for the bending of 8 layers C/Epoxy

The stiffness used in the simulation results from Pam-Form presented in this report are thus based on the large strain regime of the bending test, without the use of any viscous effects. This gave satisfying simulation results and is therefore left unchanged. In AniForm it is implemented with the constant viscosity.

3.4.3. Characterization conclusions

The characterization measurements performed on the C/Epoxy at hand were relatively successful. It appeared possible to fabricate specimens for tests that were originally developed for thermoplastic composites. Also measurements can be performed at the forming temperature and for the measurements times considered without this material showing any signs of significant cure. The curves obtained from the measurements show similarities to curves measured on thermoplastic composites. The fitting procedures previously developed can also be used on the data obtained.

Implementing the obtained values in Pam-Form deemed difficult if not impossible. The values measured for shear were therefore not used in Pam-Form. The values for bending were implemented without viscosity. The measured values will later be implemented and used in AniForm without problems. It is noted that the measurement methods used were partly developed in works related to the AniForm software. The measurement methods proposed for the Pam-Form software are however not applicable to UD prepregs.

3.5. Simulation results

The process in which a rubber membrane in a rotating frame, with a tacky composite stack stuck to it and which is formed under vacuum can be simulated using Pam-Form. The first goal of this exercise was thereby met. The input has to be very carefully chosen and numerical solutions were used to obtain a stable simulation. A summary of what the process simulation looks like is given using the images below in which the membrane was made transparent for clarity:

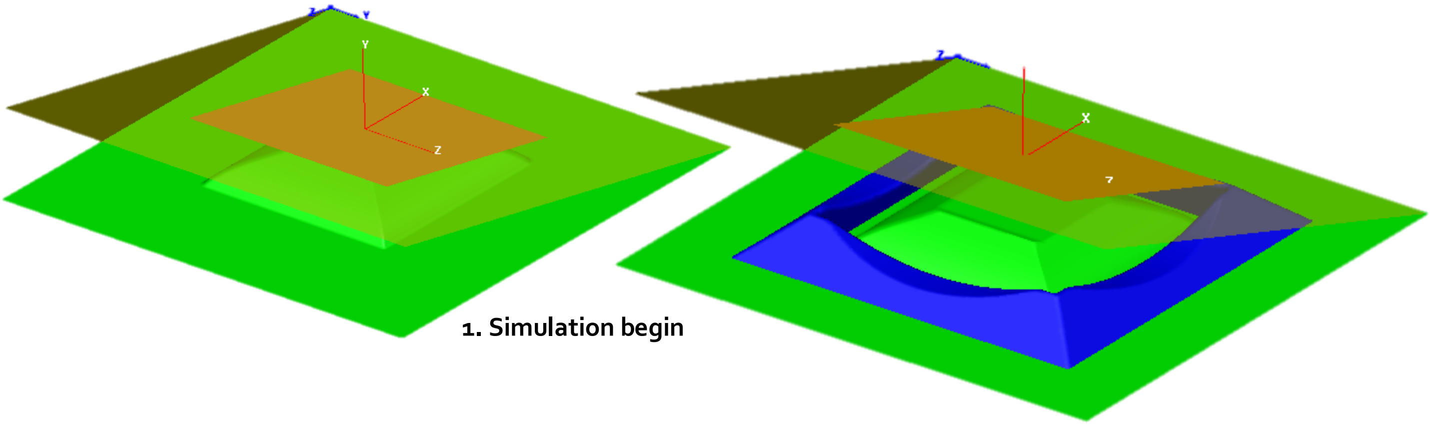

1. Simulation begin

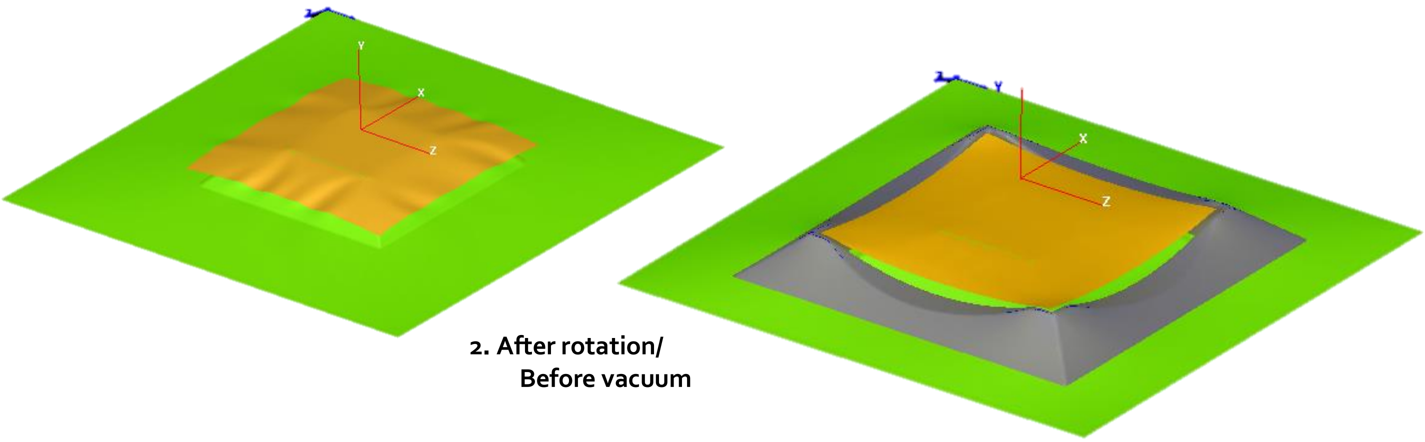

2. After rotation/
Before vacuum

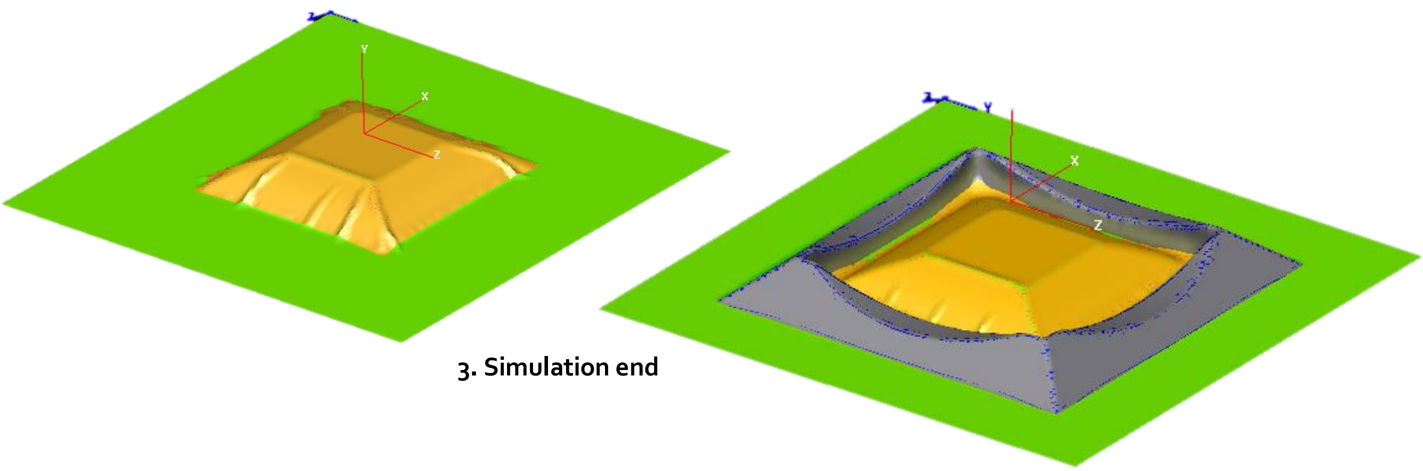

3. Simulation end

The forming using the vacuum and the membrane can also be studied as is illustrated using the images below in which the membrane is made transparent for clarity. These results enable the viewing of the details in the real forming stage.

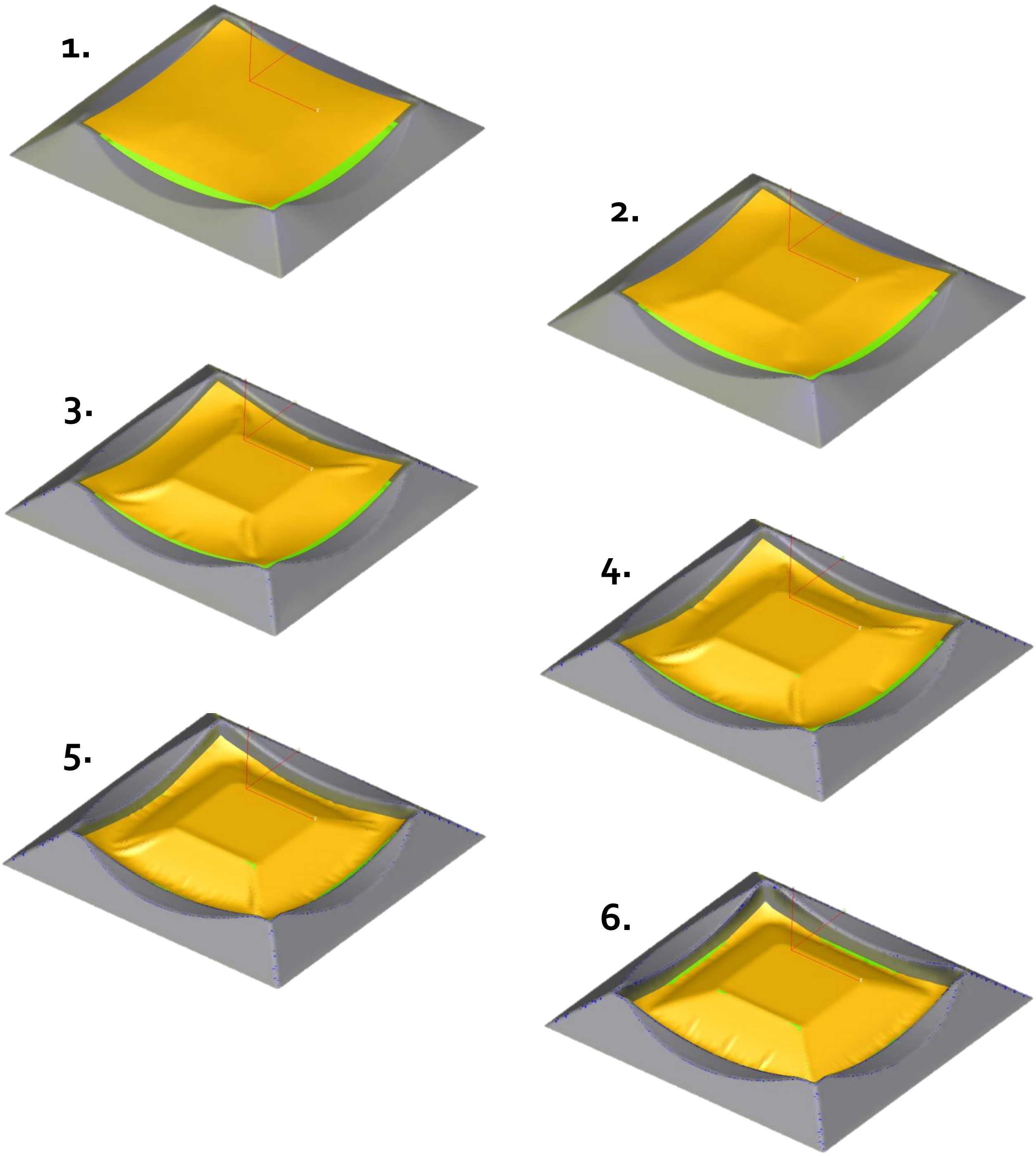

3.5.1. Results for Pam-Form

The results for preforming both types of stacks onto the mould geometry, with and without the foam tooling, is shown in Figure 15. It is observed that the wrinkling present is the simulations without foam is not present is the simulations with foam. This is in direct agreement to reality. The wrinkling in the +45/-45 forming is less than in the 0/90 forming, however the location of the wrinkles is analogue. It is noted that these results were obtained using altered values for in-plane shear to match what is seen in reality.

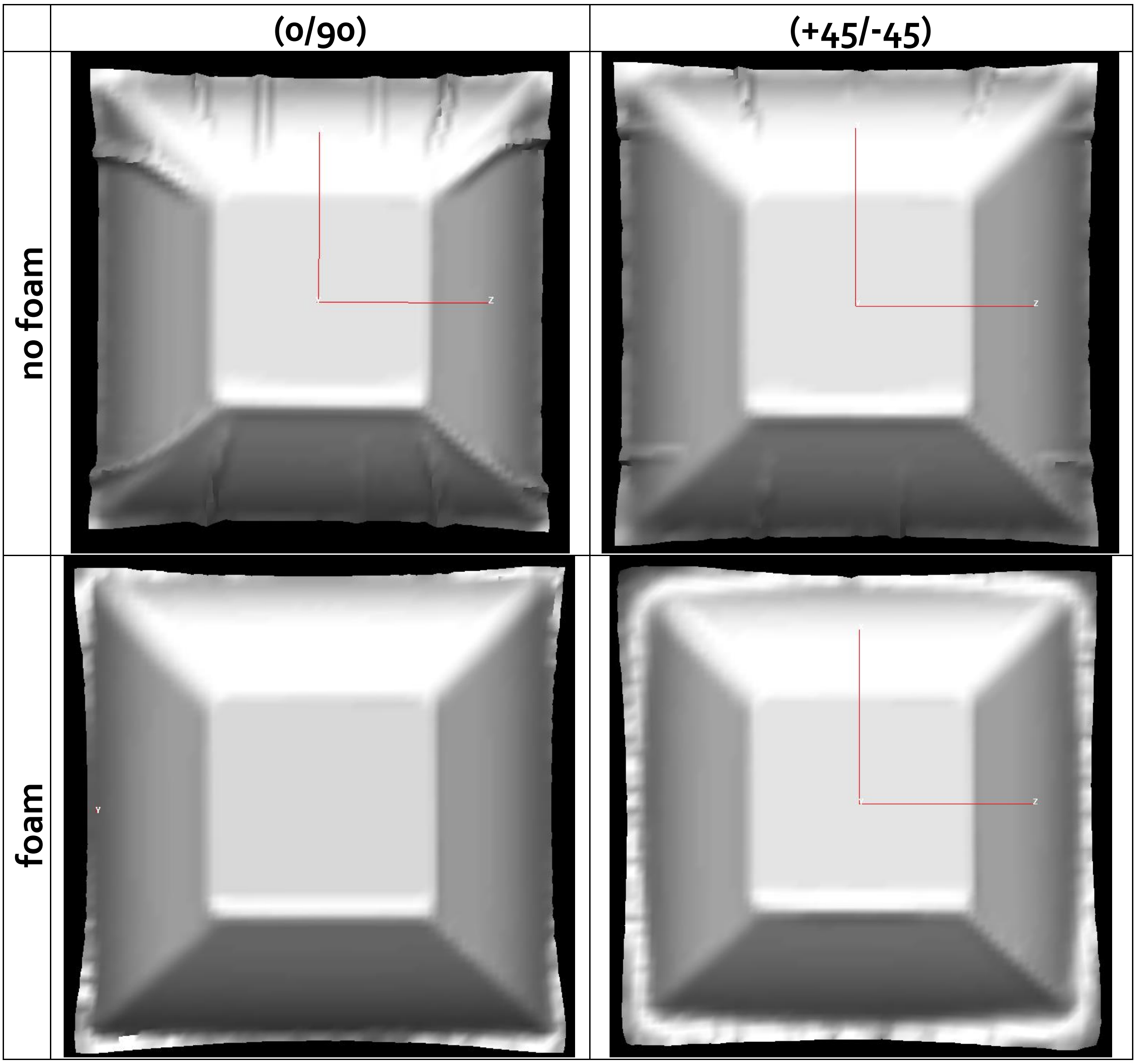

Figure 15: Simulation results for 0/90 and +45/-45, with and without foam tooling.

As already mentioned above the parts formed with the foam tooling show no wrinkles in reality and simulation. This therefore verifies those results. The only material that is available for comparison without the foam is the 0/90 stacking. Pictures of reality and simulation are shown in Figure 16. The wrinkles in real are enhanced using red lines for clarity.

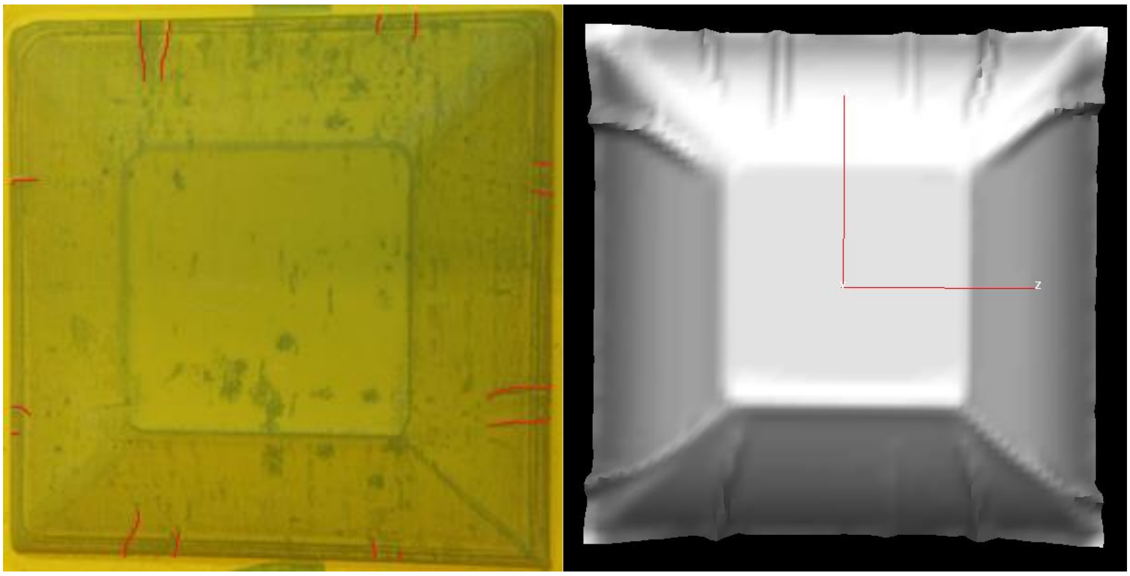

Figure 16: Comparison between forming of 0/90 without foam in the real and in simulation.

The wrinkles obtained in the simulation using Pam-Form appear to be different in shape than that in the real process, however the location and number seem to match rather well. In the simulation the wrinkling on the bottom of the image is different from that at the top of the image, this is not observed in reality. It is noted that the temperature in the real process is different from that of the measurement temperature.

4. Preforming of C/Epoxy UD prepreg using a flexible membrane – simulations in AniForm

This chapter handles the simulations done in AniForm on the same preforming process as in the previous chapter. For an introduction on the process the reader is referred to section 2 of this report.

AniForm was solely developed for doing simulations on composite forming and its numerical structure and programming are fundamentally different for that of Pam-Form. For these reasons it is interesting to make a comparison of both software's using this preform process. This chapter will highlight both the differences in workflow as for results between both sets of simulations.

4.1. Setting up the simulation in AniForm

A simulation in AniForm is always based on triangular meshes, this is contrast to Pam-Form where quadrilaterals are preferred. Therefore the tooling geometry was re-meshed with triangular elements, this time the element size was made curvature dependent since the tools are used for contact. Laminates even need special attention since element edges have to be aligned with the fibre directions of the laminate. The laminate was therefore meshed in a special way to accompany 0,90,45 and -45 degrees directions. Images for the meshes used are shown in Figure 17.

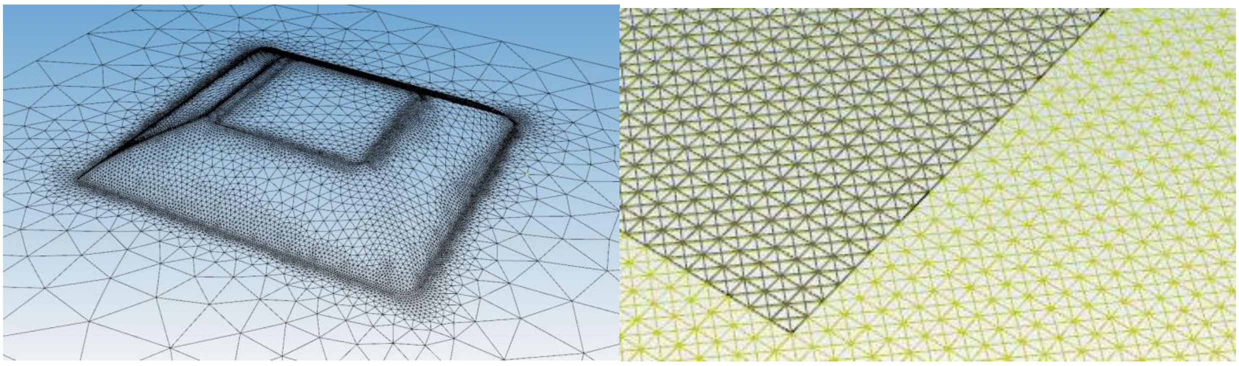

Figure 17: Meshes used for AniForm calculations.

The layup is a combination of material models for in-plane and bending, fibre directions, ply thickness and contact models. This is all provided in a single overview. The layup of the laminate is then assigned to a single layer mesh in the model. Upon simulation initiation additional meshes are created for each layer and all models are automatically applied. Due to this automatic mesh building for the laminate the positioning of the laminate mesh is crucial. The positioning should be such that the top laminate layer is in contact with the membrane upon simulation start. Large penetrations upon start however are unwanted.

Contact is also setup between laminate and tooling. Contact models are provided by the layup. Since the membrane is deformable it is not considered tooling in AniForm, therefore the contact models between laminate and membrane have to be added by hand later. Contact between laminates is also defined in the layup and applied upon initialization.

After applying most settings in the GUI tool PrePost the simulation can be initialized so the software creates an input text file for the simulation code. This text file can then be manually altered to provide more features and flexibility.

For the simulation of the membrane preforming it is necessary to alter this input file for the following simulation features.

- The edge nodes of the membrane should be a rigid body. Therefore a new tool is made using these nodes. The rigid body then also has a rotational degree of freedom which can be used to simulate the rotating of the frame.
- An additional contact between the membrane and the laminate has to be added since it was not possible before.
- Both the rotation and the pressure loading cases have to be input manually. The rotation because of the new tool added and the pressure since it is only available manually.

Other typical cases that would be added manually are gravity, springs, boundary conditions or loadings on nodes etc.

Using the adapted input file the simulation can be restarted. AniForm is based on implicit finite element method and will then solve the simulation using iterations and increments. Each increment can be scaled since loading is linear, therefore it is able to solve the easy parts at a fast pace and the more difficult parts somewhat slower. Each iteration the criteria of force balance and change in position are used to check if the current solution is convergent. More on how to influence the solving behaviour is given in a later section.

4.2. Membrane material model

In section 3.2 a model for the membrane was discussed in Pam-Form. It was shown that due to stability issues the elastic modulus as well as the constitutive description were limited. Model flexibility was not great enough to allow for a good modelling based on measurements or real values.

A constitutive model often used for rubbers and available in AniForm is the Mooney-Rivlin constitutive relation. In AniForm it is implemented as:

$$\sigma = {}^{1}/_{J}\left(C_{10} \cdot (B - I) + C_{01} \cdot (B^{-1} - I)\right)$$

Where σ is the Cauchy stress tensor, J the jacobian of the deformation tensor F, I the 3rd order unity tensor and B is the Left Cauchy-Green strain tensor. The two parameters C are used for fitting the material model.

In order to fit the parameters in the Mooney-Rivlin model it will be compared to material tests. These tests were conducted in approximation of DIN53504 for the tensile testing of thermoplastic rubbers. In the preforming process a biaxial loading of the membrane is to be expected and hence a biaxial measurement would be the test of choice. The tensile test was however still performed for the simple reason that better measuring techniques were not available.

The geometry for the tensile test can be seen in Figure 18. This geometry was the only one for which tooling was available. The thickness of the material could not be realized according to norm specifications.

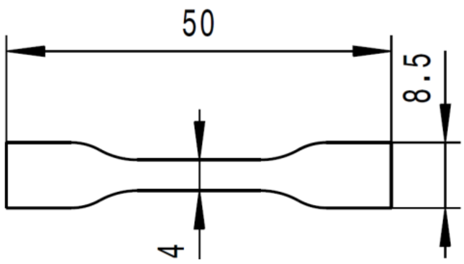

Figure 18: Overall dimensions of the testing geometry.

A typical force-displacement diagram can be found in Figure 19. Note that this curve was determined at room temperature for ease of testing. Elastic modulus of rubbers is known to increase with temperature, this is neglected here. The six specimens tested showed no difference in behavior for the beginning of the curve. Since specimens were punched in two directions it is apparent that elastic properties are not dependent on any direction in the material. Specimen failure occurred under the clamping and can therefore not be used as a result. Since the goal of these material tests is the mapping of material parameters on the beginning of the curve, the strain hardening or failure is not important.

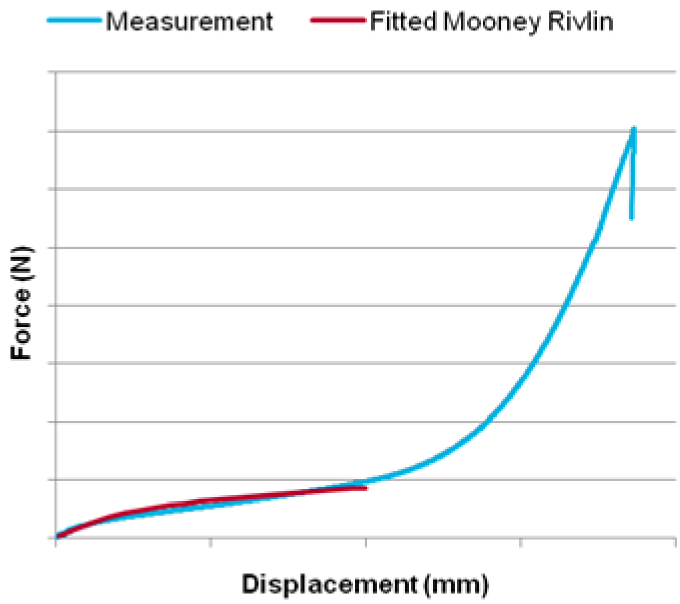

Figure 19: Fitted Mooney-Rivlin model on the force-displacement diagram of the rubber at hand.

The 2 parameter Mooney-Rivlin is known to provide good fitting in the beginning of these curves. Fitting the material values was done using a simulation of the test in AniForm and manually changing the material values. The regime up to 300% strain was used for this purpose. The final result of this exercise is shown in Figure 19.

The two parameter Mooney-Rivlin seems to fit the data up to 300% strain in good agreement. Other material models are needed if the strain hardening and failure behavior are to be included.

4.3. Optimizing simulation times

Having influence on the convergence/solving behaviour of implicit solvers is not as straightforward as for explicit solvers. For this project it was however researched and some guidelines have been setup. These guidelines helped in this particular case to reduce calculation times, should however be considered as advice and not as rules for future projects.

These methods were adopted:

- Purely elastic material models will show highly under-damped dynamic behaviour. This could results in higher speeds and strain rates, making the displacements hard to convergence. Higher speeds could also lead to difficulty upon contact initialization. Adding damping in the material in the form of a viscous material model will help to overcome these issues. The viscosity value has to be chosen such that is doesn't influence the overall deformation too much. In reality every material will have some damping effects, which also allows the use of this solution.
- The previous point is similarly valid for contact models, both normal and tangential behaviours. In contact a viscous or a damping model added could help to soften the contact and making it easier to solve.
- Also related to dynamic behaviour are the mass and inertia effects. Increasing these will smoothen the movements, making for easier solving. Thereby it is also known that the inertia values can be increased significantly without influencing the overall behaviour. Again care has to be taken that the overall behaviour is not altered by these changes.
- When contact is present upon calculation initialization (like in the preforming model) it might be preferable to start the calculation with a very small contact penetration instead of none. With this solution it is made sure that the solver doesn't have to seek contact in the first few increments.
- The size of the first increment can be altered to enable a smooth start for the solver. When calculation gets easier later it will scale the increments appropriately.
- A last resort option is always to use a bigger mesh size, but often this is unwanted. In the case of the preforming process it was chosen to use a mesh wherein element edges were aligned to both 0/90 and 45/-45 direction. Supplying two different meshes for the calculations would enable for more efficient meshing.
- Another last resort option is for contact meshes made with less elements or made more efficient. However, often unwanted.
- A solution that is not advised is to alter the unbalance values used to check convergence in each iteration. Altering these values could lead to another solution path and therefore a bad answer. The advantage of an implicit solver is then also lost.

4.4. Simulation results for AniForm

Similar to the presentation of the Pam-Form results the results obtained from AniForm are presented in Figure 20. These results are obtained using the measurements on the prepreg and the membrane. The results show that some small wrinkling is observed for the no-foam 0/90 case. All other models show no wrinkling. This finding is similar to reality in which the foam tooling enables failure free forming of the prepreg.

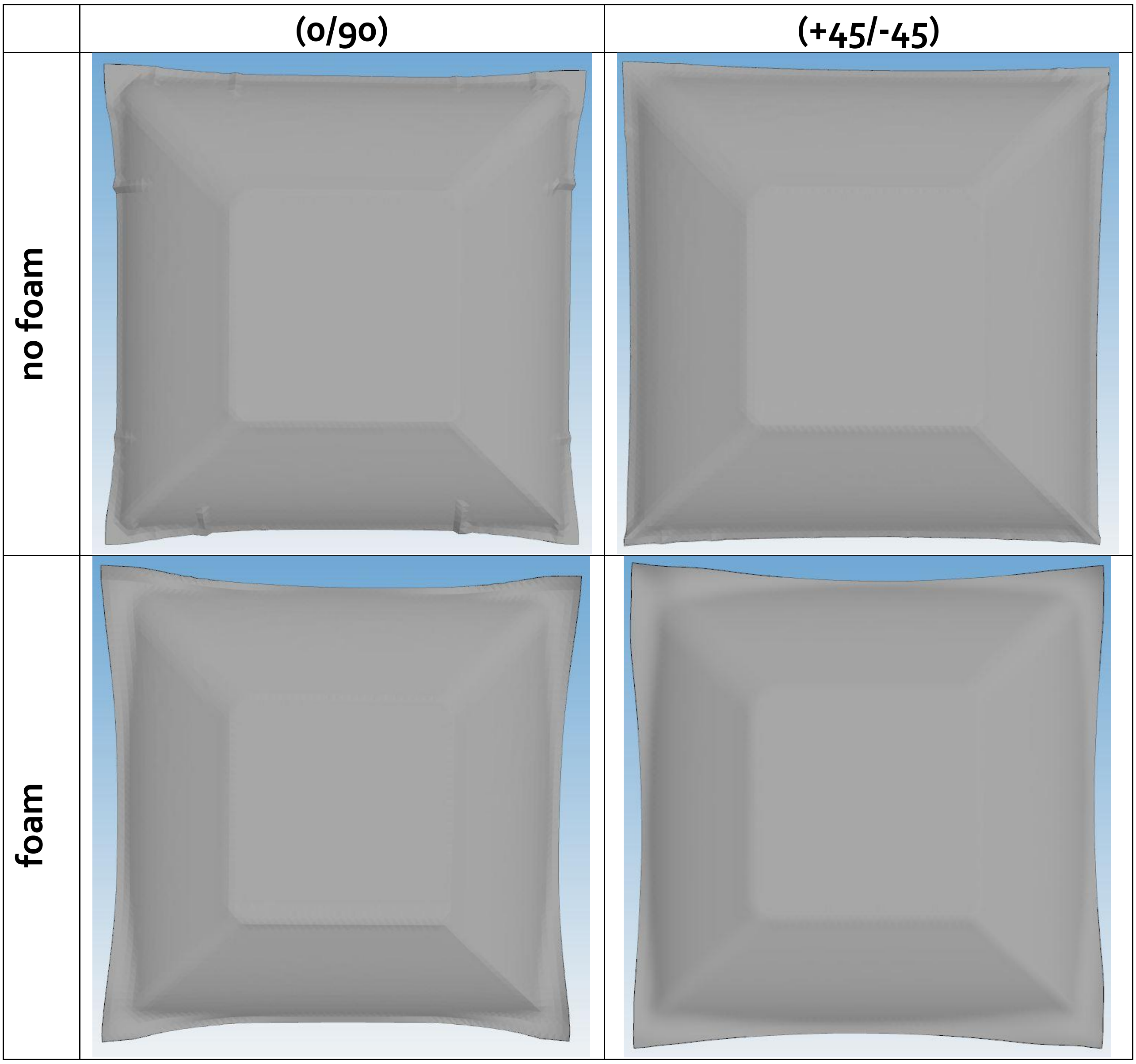

Figure 20: Simulation results for forming 0/90 and +45/-45, with and without foam tooling.

For the case of 0/90 without foam it is compared to the real process in Figure 21. It is observed that the shape and number of wrinkles is not in agreement between simulation and real process. The location of the wrinkles is predicted rather well. It is however noted that the temperature in the real process was lower than the temperature at which the material data was calibrated, making this comparison again inconclusive on the quality of the simulation model used.

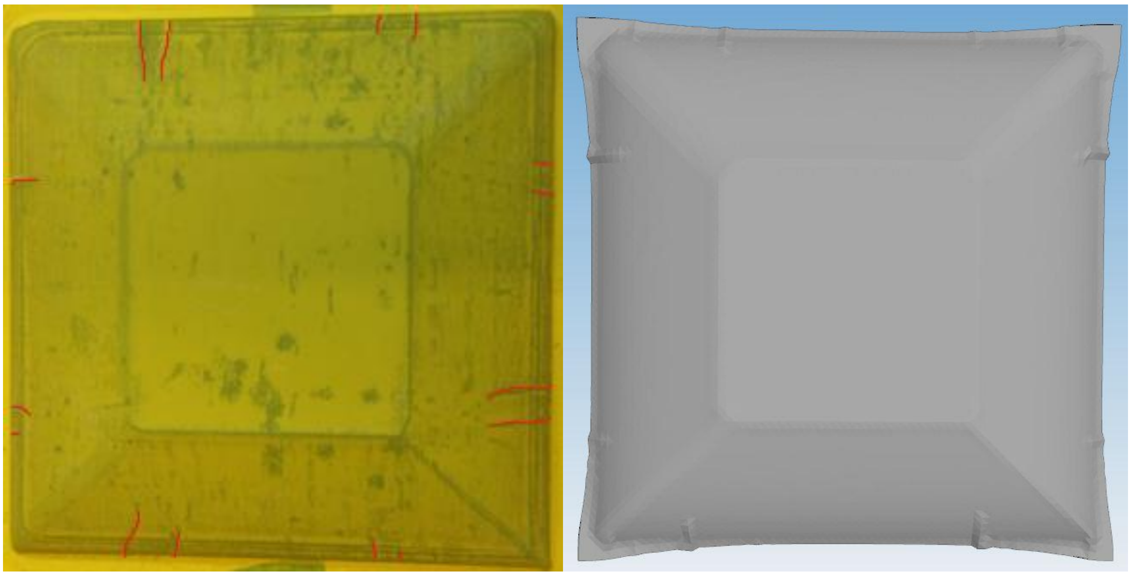

Figure 21: Comparison for forming of 0/90 without foam between simulation and the real process.

5. Conclusions on process simulations for the Preforming of C/Epoxy UD prepreg.

- Results were obtained in both attempt to model the preforming process using a flexible membrane and C/Epoxy UD prepreg. The models for both software packages were however very different and also gave very different results.
- The in-plane shear and out of plane bending properties of the UD prepreg were measured. Implementation of the characterization measurements in Pam-Form proved difficult due to viscosity values. An attempt to estimate different input values is difficult but gives results. The measurements done were related to the work of AniForm and could therefore be implemented directly. Values needed no altering in AniForm to obtain satisfying results.
- The material model used for the flexible membrane had a significant influence on simulation results. The material model for a rubber in Pam-Form could not be used due to stability issues. Another material model with adapted values was used, but left little room for adjustments. In AniForm a model often used for rubbers was adopted with the help of datasheet values. No verification of the rubber model was done.
- In both software packages some additional numerical solutions were used to positively influence calculation times, without changing the outcome. The solutions used were based on experience and included: damping in various forms, contact adjustment, additional material modelling and changing inertia effect. These optimization attempt will however be different for all other geometries and processes and can therefore only be seen as guidelines.
- A clear difference in the simulation software is that one is based on explicit methods and the other on implicit methods. In explicit analysis the calculation method is more transparent, but the user has to be aware of stability issues and the error made in the simulation results. The calculation in implicit method is not as transparent but if an answer is obtained, it at least satisfies basic engineering rules like force balance, making it more likely correct.
  No comparison in calculation times can be made and therefore no conclusion can be drawn on this subject.
- Another difference in the software is the quad/triangular element and the rule in AniForm that element edges need aligning with fibre directions. No clear advantages were found in this study to use either, these simulations were inconclusive on this subject.
- The workflow in Pam-Form is very different from that of AniForm. The author however did not find any problems concerning pre- and post-processing, some tasks were however easier in either software.

6. Analysis of methods to reduce wrinkling in press forming using simulation in Pam-Form.

In order to analyse the membrane forming process it will be compare to press forming with metal tooling. Often these forming processes are also optimized using different methods to prevent wrinkling. First a simulation without any optimization method is used to have a base line and it is compared to the membrane forming simulation. Thereafter three different methods are used to minimize wrinkling: A pulling force is applied, spring elements are applied and blank holders are tested.

6.1. Press forming with rigid tooling

A simulation is set up with rigid tooling for a [0,90] layup. Mesh size is the same as in simulations for the membrane. The simulations with and without gravity show no significant difference. The result just before the tooling is closed is showed in Figure 22. The result shows significant wrinkling, which is likely to show up in the final product. Therefore the press forming without any aid in wrinkling prevention is not a good process for this tooling geometry, layup and material combination.

A direct comparison to the membrane preforming already shows differences. It is observed in the membrane forming that the wrinkling, if present, is more localized and larger in size. In forming using rigid tooling relatively many wrinkles are observed over a large area of the part, however these wrinkles seem less severe than in membrane forming.

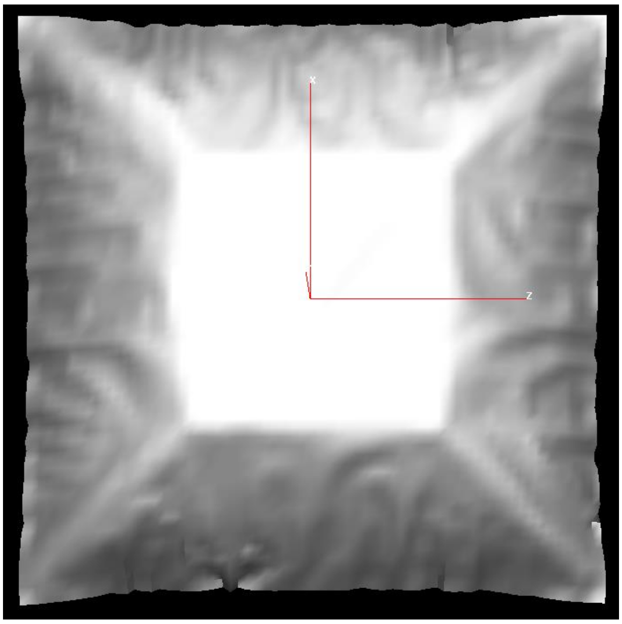

Figure 22: Forming result using rigid tooling at 90% forming.

6.2. Press forming with wrinkling reduction methods

The [0,90] layup was chosen since for this case the solution of reducing wrinkling is well known. Applying a force at the corners outwards should prevent wrinkling. This force is applied in simulation using three different methods. First a force is directly applied, then this force is supplied using spring elements and finally friction forces induced by blank holders are used. This is schematically shown in Figure 23.

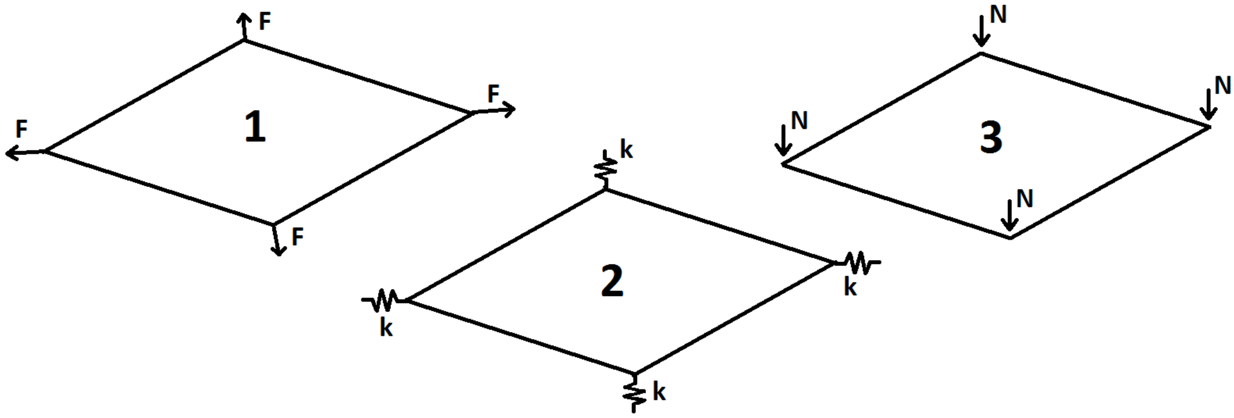

Figure 23: Three methods of reducing wrinkles.

6.2.1. Wrinkling reduction quantitative analysis

To analyse the amount of wrinkling the local curvature of the composite formed at 85% is compared to the curvature of the tooling. This curvature difference in the nodes is then averaged to obtain the element value. These are averaged while weighted with its surface area as in:

$$\zeta = \frac{1}{A} \sum A_i \cdot K_i^E$$

In which **A** is the total surface area, **A**$_i$ the element surface area and **K**$_i^E$ the averaged curvature difference from the nodes of the element. ζ is then a number that represents the amount of wrinkling. This procedure was also used by Haanappel (3) to quantify wrinkles for a parameter study. The procedure used for determining the curvature comes from Dong and Wang (5). Therein the mean curvature was modified to give a nonzero value in case of a saddle point by using:

$$K_i = {}^1\!/_2\,(|\kappa_I| + |\kappa_{II}|)$$

Figure 24 shows the analysis used on two example blanks. The left has more wrinkles then the right figure and the values of zeta also corresponds to this observation.

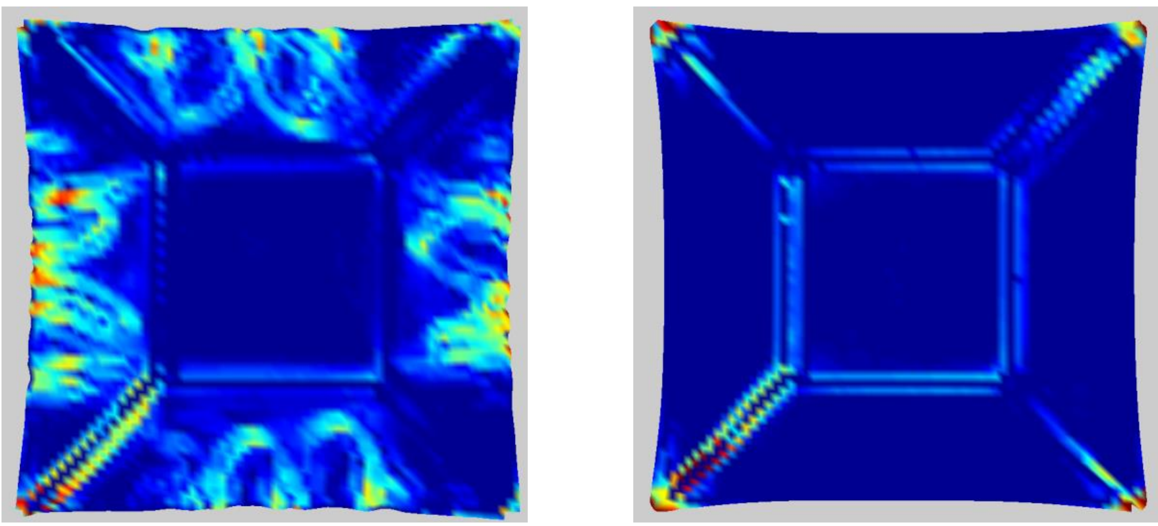

Figure 24: Composite formed at 85% curvature analysis. The left shows a lot of wrinkles and has a value of zeta 0.0068. The right corresponds nicely to the tooling curvature and has a value zeta of 0.0003.

6.2.2. Press forming with corner forces

First a force is applied on the corners of the blank while it is formed, this should minimize wrinkling. Since the force is applied rapidly in the beginning of the simulation some convergence issues can arise. To minimize these problems the corner element was made 10x stiffer than the rest of the composite to introduce the force properly. A simulation with 0N of force was conducted and compared to check the simulation validity. Thereafter various simulations were conducted with increased force values. The isometric view results for each simulation can be found in the appendix.

Here a brief summary is given using Figure 25. This plot shows that the wrinkling parameter zeta decreases when the force on the corners is increased. For the parameters used a force of about 100 N already minimizes wrinkling. If such a force can really be applied is not topic of this investigation.

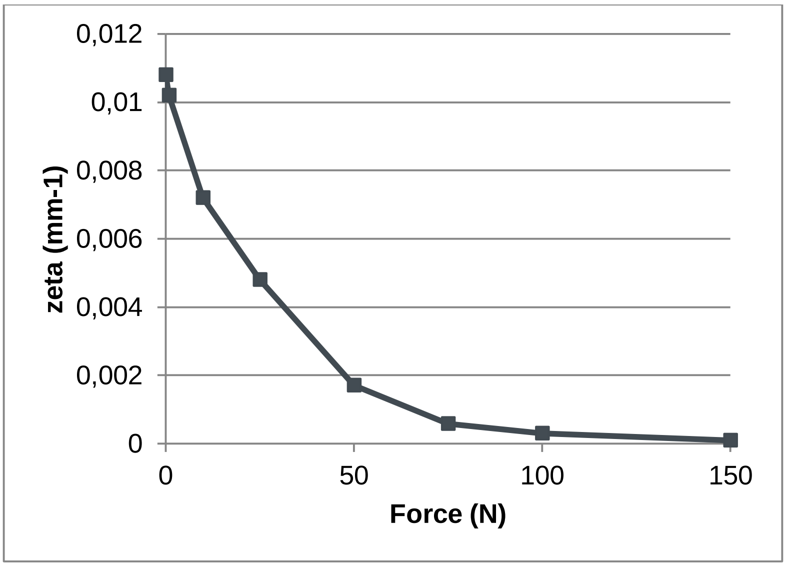

Figure 25: Plot of the wrinkling parameter zeta versus the applied force at the corners.

6.2.3. Press forming with springs at the corners.

Springs are attached to the corners of the blank. Again the corner elements have increased stiffness for stability reasons. The springs have no pretention and an initial length of 50 mm. As the forming progresses the corners are drawn inward and will tension the springs. Various simulations with increased spring stiffness were conducted. The isometric view images can be found in the appendix.

A summary of the results is given in Figure 26. The wrinkling parameter zeta shows a decrease when increasing the spring stiffness. After 125 N/mm the wrinkling remains constant and does not decrease to zero. Such high stiffness' are not a very realistic case, however it is noted that a more compliant spring with pre-tension could be a realistic method similar to applying a force on the corners like in the previous analysis.

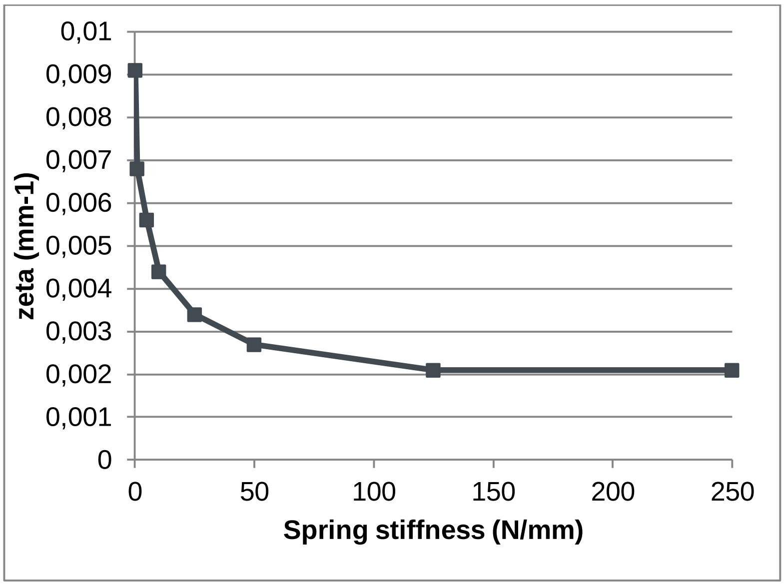

Figure 26: Plot of the wrinkling parameter zeta versus the spring stiffness at the corners.

6.2.4. Press forming using blank holders

Blank holders are also often applied to decrease wrinkling in a formed part. The blank holders in this case are only modelled at the corners. An image of the geometry used to simulate the blank holders is shown in Figure 27.Again a simulation without a normal force on the blank holders was conducted and gave the same results as normal pressing. During various simulations the normal force on the blank holders was increased. The coulomb friction with coefficient 0.3 will then provide a friction force on the corners, which will decrease wrinkling. In the appendix the isometric view images are given.

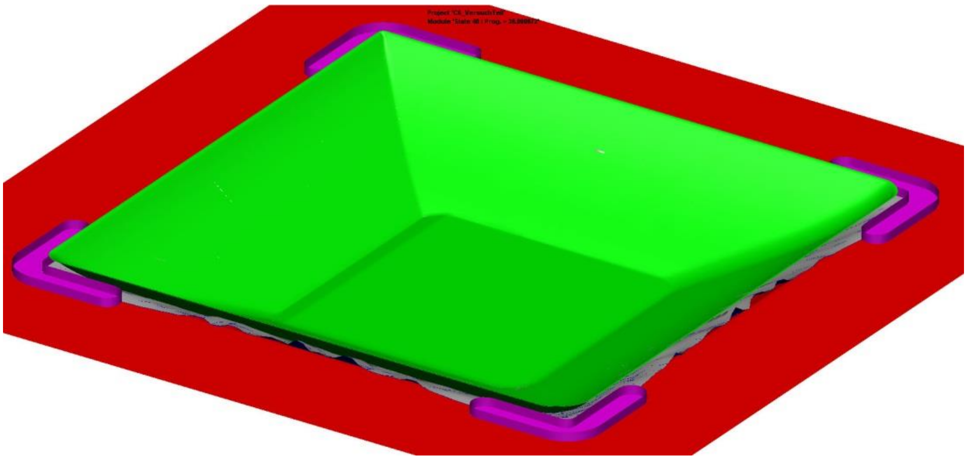

Figure 27: Geometry used to simulate a process using blank holders at the corners.

Here a summary of the results is given in Figure 28. This plot shows constant wrinkling up to 1kN normal force after which it decreases significantly up to 10kN. The wrinkling was not decreased much by increasing the force to 40kN.

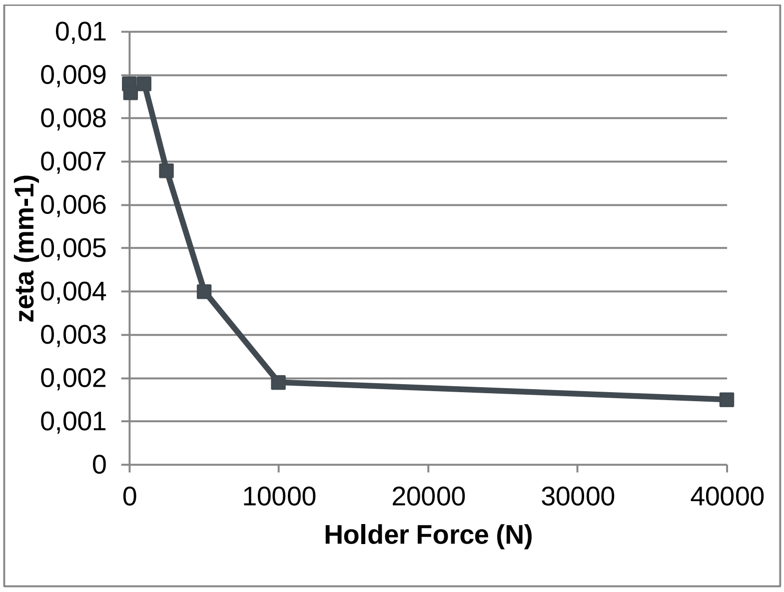

Figure 28: Plot of the wrinkling parameter zeta versus the normal force of the blank holders.

6.2.5. Press forming with limited corner movement

The corner nodes can also be prevented from movement in plane to simulate a pulling force. This results shown indeed no wrinkling but introduces significant and unrealistic strains in the composite, this results is therefore left out of this study.

6.3. Concluding on wrinkling reduction

Three methods were used to minimize wrinkling on the press formed part. All three methods used show improvement in a certain range of input values. The force at the corners is the only method found to prevent all wrinkles. The spring and blank holders decrease the amount of wrinkles but then seem to stabilize at a certain amount. This simulative study however cannot conclude if the values are also realistic in practical use.

When comparing the discussed methods to the membrane forming it is noted that both methods are capable of reducing or eliminating wrinkling. The membrane forming has the advantage that it is not introducing loads locally and therefore has less chance of ply split or other force related problems. The disadvantage of the membrane forming is that it is unknown how it influences wrinkling and draping and therefore the optimization for different part geometries might be more difficult.

Bibliography

1. *Mechanical experimental characterization and numerical modelling of an unfilled silicone rubber.* **L. Meunier, G. Chagon, D. Favier, L. Orgéas and O. Vacher.** April 2008, Polymer Testing 27, pp. 765-777.

2. *Uber die partiellen differenzengleichungen der mathematischen physik.* **R. Courant, K. Friedrichs and H. Lewy.** 100, 1928, Mathematische Annalen, pp. 32-74.

3. *Shear characterisation of uni-directional fibre reinforced thermoplastic melts by means of torsion.* **S.P. Haanappel, R. Akkerman.** February 2014, Composites: Part A, Vol. 56, pp. 8-26.

4. *Bending characterization of UD composites.* **U. Sachs, R. Akkerman, S.P. Haanappel.** May 2014, Key Engineering Materials, Vol. 611, pp. 399-406.

5. **Dong Chen-shi, Wang Guo-zhao.** Curvatures estimation on triangular mesh. *Journal of Zheijang University SCIENCE.* 6A, 2005, pp. 128-136.

6. *Rheology of polypropylene in solid state.* **P. Duffo, B.Monasse, J.M. Haudin, C. G'Sell, A. Dahoun.** June 1994, Journal of Material Science, Vol. 30, pp. 701-711.

7. **903, British Standard.** Methods of testing vulcanised rubber Part 19 (1950) and 7A (1957).

8. ***http://en.wikipedia.org/wiki/Mooney%E2%80%93Rivlin_solid.***

Appendix A: Images of wrinkling reduction

By applying force on the corners:

0 N	50 N
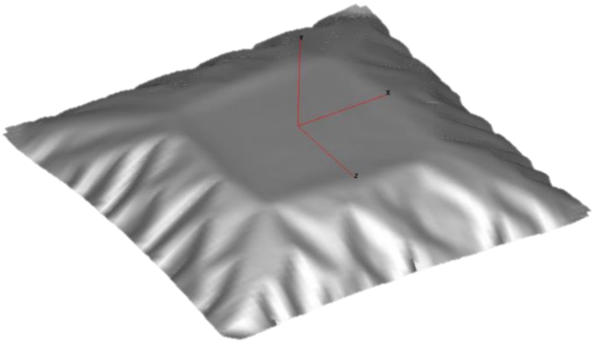	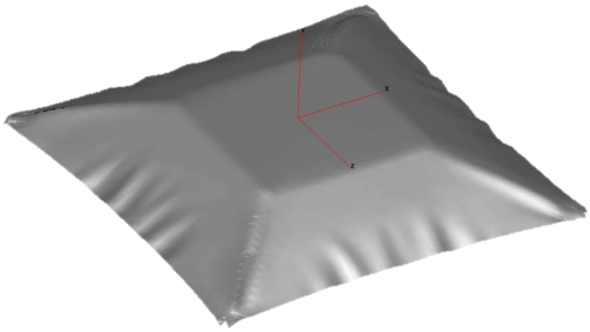
1 N	100 N
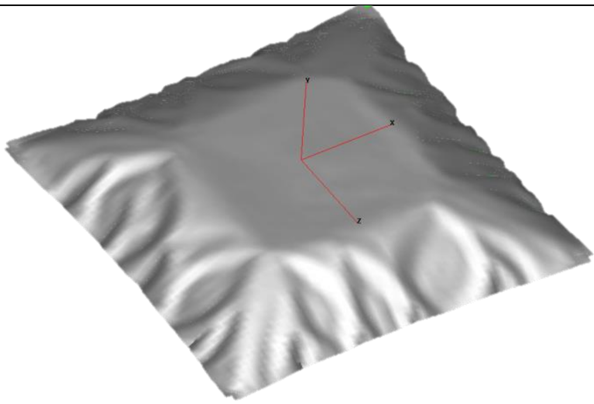	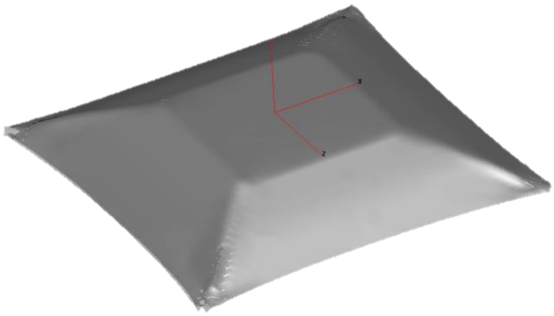
10 N	150 N
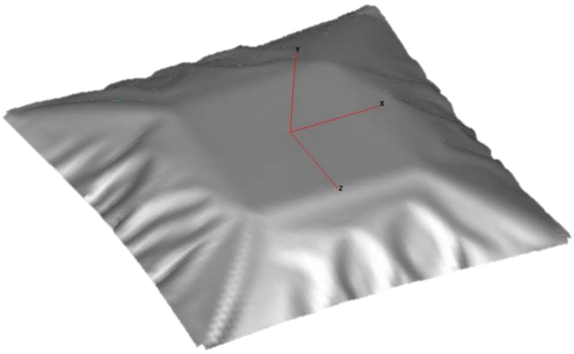	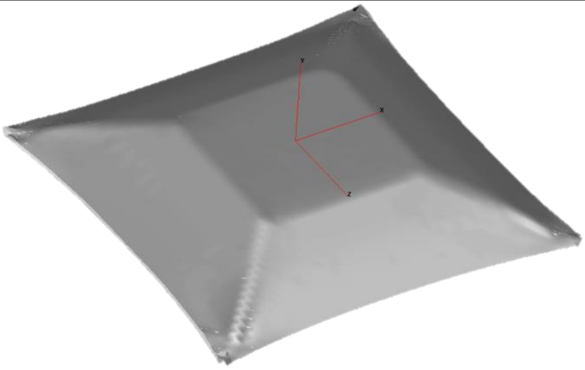

Spring connected to the corners:

1 N/mm	25 N/mm
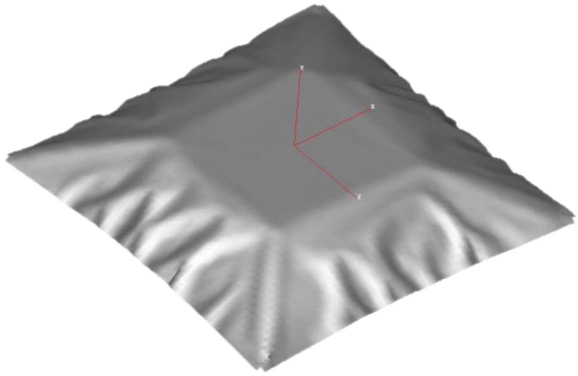	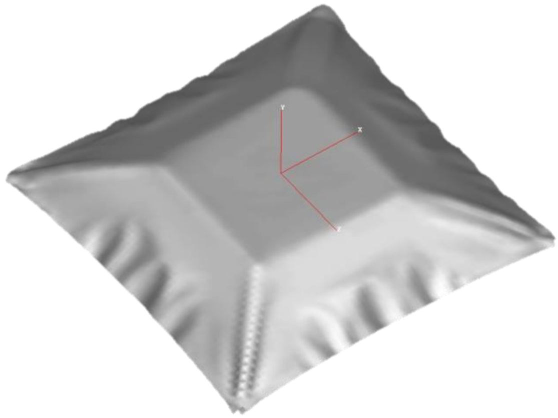
5 N/mm	50 N/mm
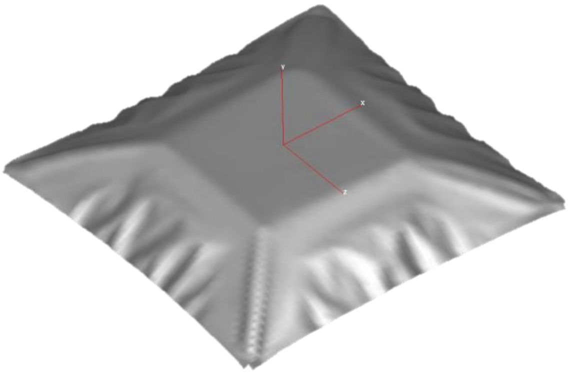	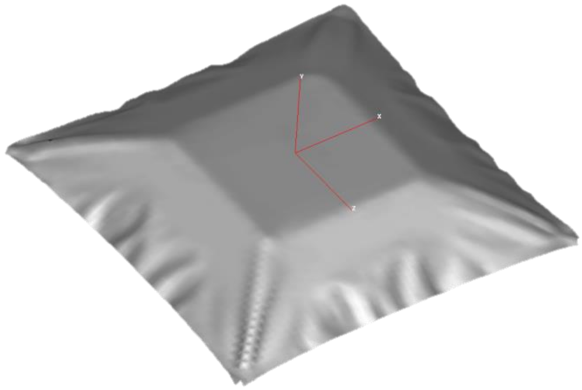
10 N/mm	125 N/mm
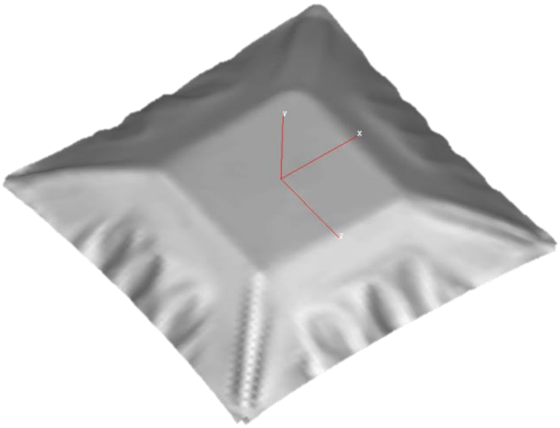	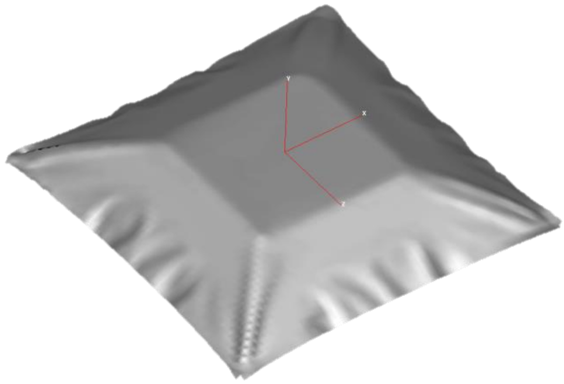

Using a blank holder at the corners:

0.1 kN	5 kN
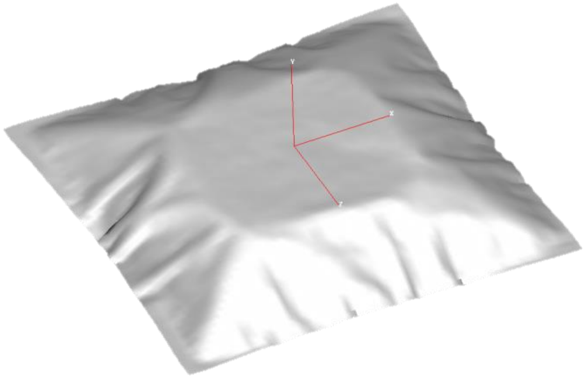	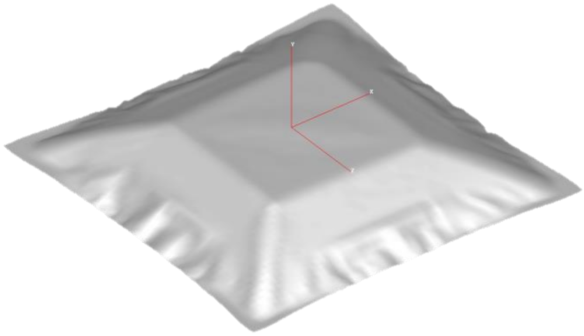
1 kN	10 kN
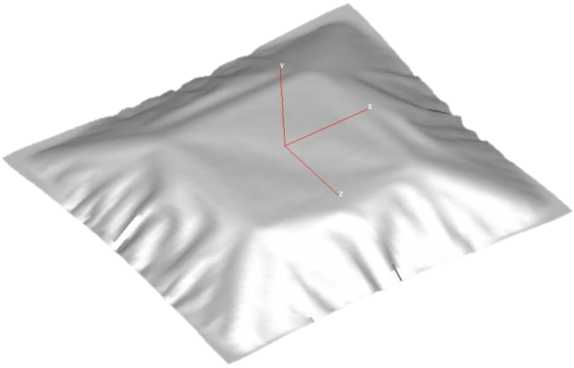	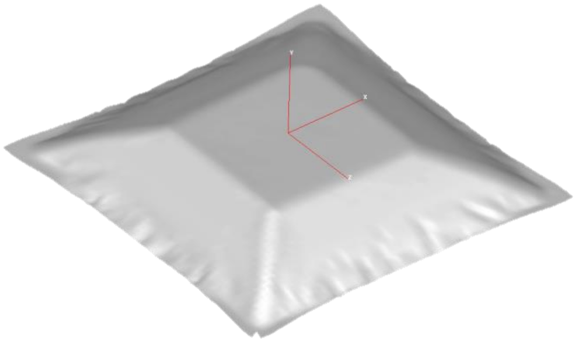
2.5 kN	40 kN